



Published in final edited form as:

Endocrinology. 2007 November ; 148(11): 5487–5495. doi:10.1210/en.2007-0775.

A Role for Androgens in Regulating Circadian Behavior and the Suprachiasmatic Nucleus

Iliia N. Karatsoreos, Alice Wang, Jasmine Sasanian, and Rae Silver

Departments of Psychology (I.N.K., A.W., R.S.) and Anatomy and Cell Biology (R.S.), Columbia University, New York, New York 10032; and Department of Psychology (J.S., R.S.), Barnard College, New York, New York 10027

Abstract

The suprachiasmatic nucleus (SCN) of the hypothalamus is the locus of a master circadian clock controlling behavioral and physiological rhythms, including rhythmic secretion of gonadal hormones. Gonadectomy results in marked alteration of circadian behaviors, including lengthened free-running period, decreased precision of daily onset of running, and elimination of early-evening but not late-night activity bouts. Androgen replacement restores these responses. These aspects of rhythmicity are thought to be regulated by the brain clock, although the site of androgen action remains unknown. Anatomically, the rodent SCN is composed of a ventrolateral core and a dorsomedial shell, and the present studies show that androgen receptors (AR) are localized to the ventrolateral core SCN. Using a transgenic mouse bearing dual reporter molecules driven by the AR targeted to both membrane and nucleus, we find that projections of AR-containing cells form a dense plexus in the core, with their fibers appearing to exit the SCN dorsally. In a second transgenic strain, in which the retinorecipient gastrin-releasing peptide cells express a green fluorescent protein reporter, we show that gastrin-releasing peptide cells contain AR. Through immunocytochemistry, we also show that SCN AR cells express FOS after a light pulse. Importantly, gonadectomy reduces the FOS response after a phase-shifting light pulse, whereas androgen replacement restores levels to those in intact animals. Taken together, the results support previous findings of a hypothalamic neuroendocrine feedback loop. As such, the SCN regulates circadian rhythms in gonadal hormone secretion, and in turn, androgens act on their receptors within the SCN to alter circadian function.

In mammals, the master circadian clock is located in the bilaterally paired suprachiasmatic nuclei (SCN) of the hypothalamus and controls the period and precision of daily timing of behavior. There is substantial evidence that this brain clock does not require input from the rest of the body or from the environment to sustain rhythmicity. Individual SCN neurons studied *in vitro* as dispersed cultures are cell autonomous independent oscillators expressing circadian rhythms in electrical activity (1). Moreover, in organotypic cultures of SCN tissue, SCN neurons show circadian patterns of clock gene expression and clock protein levels (2, 3). Furthermore, the SCN tissue as a whole expresses coherent rhythms even when isolated from the rest of the brain *in vitro* (4). Nevertheless, inputs to the SCN are important in setting the phase of the clock and in modulating gene expression and neuronal activity *in vivo*.

Copyright © 2007 by The Endocrine Society

Address all correspondence and requests for reprints to: Rae Silver, Ph.D., Department of Psychology, Columbia University, 406 Schermerhorn Hall, MC5501, 1190 Amsterdam Avenue, New York, New York 10027. qr@columbia.edu.

Disclosure Statement: The authors have nothing to disclose.

Endocrinology is published monthly by The Endocrine Society (<http://www.endo-society.org>), the foremost professional society serving the endocrine community.

The SCN is anatomically and functionally heterogeneous with respect to peptidergic and neurotransmitter content, electrical activity, and gene expression patterns, although the significance of this heterogeneity is not well understood. Based on numerous anatomical and morphological features, it has been conceptualized as having a dorsomedial shell region and a ventrolateral core region (5). Although first coined in the rat, these terms have been applied to the mouse as well (6). Functional criteria support this general delineation; cells of the dorsomedial shell are rhythmic in gene expression, neuropeptide secretion, and electrical activity (7–10), and their response to light is delayed compared with core cells (11). In contrast, the ventrolateral core region bears some cells that lack detectable rhythmicity in clock genes and electrical activity and shows rapid induction of FOS and clock genes after a light pulse (9–12). It is well established that the core region receives the majority of neural afferents from the retina, the intergeniculate leaflet, and raphe nucleus (reviewed in Ref. 13). In contrast, the site of endocrine action is poorly understood, although hormonal influences and sex differences in circadian responses are well documented (14–17).

The present studies focused on androgen actions in the SCN. In male mice, there are marked behavioral effects of castration (18). After gonadectomy, mice show lengthening of free-running period, a complete loss of the activity onset bout, and a decrease in overall amount of activity. In male hamsters, surgical or photoperiodic castration (*i.e.* short-day-length-induced testicular regression and decreased plasma testosterone) results in loss of precision in onset of locomotor activity and decreased cohesion of the daily running bout (19). These responses are restored by testosterone replacement. Although the sites of androgenic hormone action on rhythmicity remain to be delineated, some of these behavioral responses, including period and precision, are thought to be controlled by the circadian pacemaker directly (20). Whether androgens act on one or both SCN subdivisions has not been explored, although scattered androgen receptor (AR) expression within the nucleus has been reported in several species (21–25). A site of action specific to one functional subdivision would be important in understanding mechanisms of androgenic action on SCN circuits. The goals of the present study were to explore the localization of AR expression in the mouse SCN, the projections of AR-containing cells, and the effect of castration and hormone replacement on SCN neuronal responses to phase-shifting light pulses.

Materials and Methods

Animals and housing

Three strains of mice were used. Male C57BL/6 mice were purchased at 45 d of age (Charles River Labs, Kingston, NY) and allowed to acclimate to the animal facility for 2 wk. All other animals were bred at the Barnard College Animal Facility. Male CalB::GFP transgenic mice on a C57 background (gift of Dr. N. Heintz, Rockefeller University) bearing a green fluorescent protein (GFP) reporter labeling gastrin-releasing peptide (GRP) cells in the SCN were used for double-labeling immunocytochemistry (ICC) studies. As previously reported (9), in the CalB::GFP mouse, all GFP cells in the SCN coexpress GRP; thus, the GFP reporter allows for the visualization of GRP cell bodies (GRP cell bodies of the SCN cannot be visualized without the use of colchicines, because dense GRP fibers obscure the GRP-containing cell somas). Mice bearing a modified AR gene (gift of Dr. N. Shah, University of California, San Francisco) were used to confirm ICC results as well as to allow visualization of AR cell projections. Briefly, these animals had a modified AR gene containing an AR-IRES-PLAP-IRES-nlacZ-CAN cassette, providing membrane-targeted placental alkaline phosphatase (PLAP) and nuclear-targeted lacZ in cells expressing the AR (26).

Animals were housed with a 12-h light, 12-h dark cycle (12:12 LD) unless otherwise noted. A dim red light allowed for animal maintenance. Animals had *ad libitum* access to food and

water and were cared for in accordance with the guidelines of Columbia University's Institutional Animal Care and Use Committee.

Gonadectomy (GDX) and hormone replacement

GDX—Mice were deeply anesthetized with ketamine (70 mg/kg, sc) and xylazine (5 mg/kg, sc), with buprenorphine (0.5 mg/kg, sc) as an analgesic. GDX was by abdominal incision and removal of both testes. Muscle and fascia were closed using surgical silk, and the overlying skin was sutured.

Steroid implants—Implants were prepared to mimic physiological levels of hormones as previously described (27, 28). Briefly, SILASTIC brand capsules (Dow Corning, Fisher Scientific, Waltham, MA; inner diameter 0.98 mm, outer diameter 2.16 mm) were filled with crystalline testosterone propionate (TP, 5 mm long) or dihydrotestosterone (DHT; 10 mm long) (TP and DHT were from Steraloids Inc., Newport, RI), sealed with SILASTIC brand glue, and allowed to dry overnight. All capsules were primed in a 37 C 0.9% saline bath for 36 h before implantation.

Experimental design

Anatomical distribution of AR within the SCN—Gonadally intact wild-type (n = 4) and AR-transgenic (n = 4) animals were used to examine the distribution of AR within the SCN as well as the projection patterns of AR-containing cells.

Delineation of core and shell

In the present study, we use the term core to refer to the regions of the SCN that contain GRP- and vasoactive intestinal polypeptide (VIP)-positive cells. In the mid-SCN, these cells occupy the central and ventral SCN (respectively, Fig. 3 in the present study and Fig. 5 in Ref. 6). The precise location of these cell groups changes depending on the antero-posterior location within the SCN (Fig. 2 in Ref. 12 and Ref. 6). We use the term shell to refer to the region of the mouse SCN that contains arginine vasopressin (AVP) cells. These cells occupy the dorsal and medial aspects of the SCN (6, 12).

SCN AR expression in LD and constant darkness (DD)—Western blots were used to assess diurnal and circadian rhythms of AR protein in the SCN. Animals were maintained in 12:12 LD, and one group was placed in DD for 2 d before the experiment and killed in DD. Animals (n = 3 per group) were killed every 4 h at zeitgeber time (ZT) or circadian time (CT) 0, 4, 8, 12, 16, and 20.

Hormonal regulation of AR-immunoreactivity (AR-ir) within the SCN—To determine the effects of GDX and androgen replacement on SCN AR expression, animals were split into three groups, intact (INT), 7 d post GDX, or GDX and treated with TP for 7 d (GDX+TP), and then killed (n = 6 per group).

Light-induced FOS in the SCN—To determine whether AR-containing SCN cells express FOS after a light pulse, INT (n = 8) animals were maintained in 12:12 LD and then transferred to DD. On the third day in DD, a 30-min light pulse (800 lux) was delivered at CT13.5 (n = 6), and animals were returned to darkness for 60 min and then killed. Control animals (n = 2) were not exposed to light and were killed at CT14.5. Because the observed effects of GDX on behavior were most pronounced at the onset of nighttime activity (CT12–18), we chose CT13.5 to test whether AR and FOS colocalize after a light pulse.

Gonadal hormone regulation of light-induced FOS in the SCN—To determine whether GDX and replacement with the nonaromatizable androgen DHT modulates the light-induced SCN FOS response, animals were assigned to one of three groups: INT (n = 12), 7 d GDX (GDX; n = 12), or 7 d GDX plus DHT (DHT; n = 12). Castrates were implanted sc with either DHT (n = 12) or a blank capsule (n = 12) and maintained in 12:12 LD for 7 d and then transferred into DD for 2 d. On the third day in DD, animals were exposed to a 30-min light pulse at either CT13.5 (n = 12) or CT21 (n = 12) or left unmanipulated (n = 6 per time point) and killed 1 h after the end of the light pulse.

Behavioral changes after castration and hormone replacement—For behavioral experiments, animals were individually housed in polypropylene cages equipped with a running wheel connected to a computer. Locomotor activity in the form of wheel revolutions was recorded continuously in 10-min bins for 2–3 months over the duration of the experiment (Dataquest, Minimitter Co. Inc., Sunriver, OR). After 2–3 wk acclimatization, animals were placed into DD. A dim red light (<1 lux) allowed for animal maintenance, and sound was masked by a white-noise generator (91 spl). After at least 3 wk in DD, one group of animals was GDX (n = 14), whereas controls (n = 4) were anesthetized without surgery. Animals were then returned to DD for at least 2 wk. After 2 wk of testing, GDX animals were implanted with a sc SILASTIC brand capsule bearing either TP (n = 6) or DHT (n = 4) or an empty capsule (n = 4). After another 2 wk, the latter group were reimplanted with TP (n = 2) or DHT (n = 2). Thus, in the behavioral studies, eight animals were tested with TP and six with DHT.

Perfusion and ICC

For ICC, animals were deeply anesthetized (pentobarbital, 200 mg/kg ip) under dim red light, their heads covered with a lightproof hood, and perfused intracardially with 50 ml saline followed by 100 ml 4% paraformaldehyde in 0.1 M phosphate buffer (PB), pH 7.3. Brains were postfixed for 4 h at 4 C and cryoprotected in 20% sucrose in 0.1 M PB overnight.

Brains were sectioned at 35 μ m on a cryostat. For single-label ICC, free-floating sections were incubated in 1% hydrogen peroxide, washed three times for 10 min each in PBS, incubated in normal goat serum for 1 h, and placed in anti-AR made in rabbit primary antibody (Santa Cruz Biotechnology, Santa Cruz, CA; 1:5000) for 48 h. Sections were then washed three times for 10 min each in PB with 1% Triton X-100, incubated in biotinylated goat antirabbit secondary (Vector Laboratories, Burlingame, CA; 1:250) for 1 h, and washed. Sections were then treated with avidin-biotin complex (ABC; Vector) for 1 h and washed. Staining was visualized with nickel chloride-enhanced diaminobenzidine (Sigma-Aldrich, St. Louis, MO). Sections were mounted on gel-coated glass slides, dehydrated in a graded series of alcohols (50–100%), and coverslipped with Permount (Fisher Scientific, Hampton, NH). For double-label ICC, free-floating sections were incubated in normal donkey serum for 1 h and then simultaneously in anti-AR made in rabbit (Santa Cruz; 1:5000) and one of the following: anti-GFP, made in chicken (Aves Labs, Tigard, OR; 1:3000), anti-AVP made in guinea pig (Peninsula Labs/Bachem, Belmont, CA; 1:5000), anti-VIP made in guinea pig (Peninsula/Bachem; 1:5000), anti-FOS made in goat (Santa Cruz, 1:10,000) for 48 h. For lacZ staining, sections were incubated in anti- β -galactosidase made in rabbit (Cortex Biochemicals, San Leandro, CA) overnight at room temperature. After the primary incubation, sections were washed three times for 10 min each with PB with 1% Triton X-100 and then placed into a donkey secondary conjugated to CY2 (antichicken for GFP, anti-guinea pig for AVP and VIP, and antigoat for FOS) or CY3 (antirabbit for AR) fluorophores (1:200; Jackson ImmunoResearch, West Grove, PA) for 1

h. Sections were washed in PBS, mounted onto gel-coated slides, and dehydrated in alcohols (as above). Coverslips were applied with Krystalon (EM Science, Gibbstown, NJ).

ICC controls for each antibody included a preadsorption and a no-primary control; staining was absent under these conditions. In addition, a second anti-AR antibody [rabbit anti-AR-PG21; Upstate USA Inc. (now part of Millipore Inc.), Charlottesville, VA] was tested using the same reagents and techniques with the same results. For lacZ staining control, brains from wild-type littermates of AR-transgenics were incubated simultaneously with transgenic tissue; no staining was observed.

For PLAP staining, 50- μ m sections were made on a vibratome, and washed three times for 10 min each in PBS. Sections were washed with PLAP buffer (0.1 M Tris, 0.1 M NaCl, 0.05 M MgCl₂) for 10 min and incubated in PLAP buffer for 45 min at 65 C to deactivate endogenous alkaline phosphatases. Sections were then incubated for 4 h in PLAP buffer with 0.2 mg/ml 5-bromo-4-chloro-3-indolyl phosphate and 1 mg/ml nitroblue tetrazolium at room temperature, washed three times for 10 min each in PBS, fixed for 10 min in 4% paraformaldehyde, and washed again for 10 min in PBS. Sections were then mounted on gel-coated slides, dehydrated in alcohols (as above), and coverslipped with Permount.

Western blotting

Animals were euthanized with CO₂ and their brains removed and placed in ice-cold saline. Using a vibratome, 400- μ m sections of hypothalamus were collected in ice-cold saline, and the SCN were harvested bilaterally with the aid of a dissecting microscope. To prepare SCN lysates, tissue was homogenized by sonication in lysis buffer (1% SDS in dH₂O with Roche complete, Mini, EDTA-free protease inhibitor cock-tail) and then incubated in a boiling water bath for 10 min. Lysates were spun in a microfuge (30 sec at 13,000 rpm) to remove insoluble material. Protein concentration of the supernatant was determined using the bicinchoninic acid method (Pierce, Rockford, IL). Lysates (5 μ g/lane) were subjected to SDS gel electrophoresis, blotted to a nitrocellulose membrane, and probed with the AR antibody (1:10,000). Proteins were visualized by chemiluminescence, according to the manufacturer's instructions (Lumiglo; Cell Signaling, Beverly, MA). Relative OD of the Western blots was measured using image analysis software (MCID, St. Catharines, Ontario, Canada). Both Santa Cruz and Upstate anti-AR antibodies were run on a Western blot of SCN cell lysates, and a specific band was observed at about 98 kDa, the molecular mass for the mouse AR (29).

Data analysis

Microscopy—Sections were examined on a Nikon Eclipse E800 microscope (Nikon, Tokyo, Japan). Images were captured with a cooled CCD camera (SPOT; Morrell, Melville, NY) and stored on a PC for subsequent analysis. PLAP and diaminobenzidine staining were used to examine projection patterns of AR cells and for the quantification of androgenic effects on receptor expression. Images were captured in 8-bit grayscale. Conventional fluorescent microscopy was used to assess colocalization of AR and GRP, VIP, AVP, and FOS and for β -galactosidase staining. Sections were examined with filters for GFP (480 \pm 20 nm) and Texas Red (560 \pm 40 nm), with each channel acquired independently, and then combined digitally using the SPOT software.

The extent of the mouse SCN is approximately 420 μ m from rostral to caudal. Sections were taken from the rostral approximately 40- to 80- μ m, middle approximately 160- to 200- μ m, and caudal approximately 320- to 360- μ m aspects of the SCN. The mid-SCN was definitively identified by its characteristic pattern of AVP staining. For quantitative analyses, a grid of 220 \times 220 μ m was centered over the mid-SCN, and all cells within this

grid were counted. Four SCNs (left and right side of two sections) were counted, and a total was calculated for each animal and then collapsed for a group average.

The colocalization of AR/GFP (GRP), VIP or AVP, and AR/FOS was examined by confocal microscopy using a Zeiss Axiovert 200M fluorescence microscope (Carl Zeiss, Thornwood, NY) with a Zeiss LSM 510-META scanning confocal attachment. Sections were excited sequentially with an argon-krypton laser using the standard excitation wavelength for CY2 and CY3. Stacked images were collected as 1- μm multitract optical sections. LSM 3.95 software (Zeiss) was used to superimpose red and green images of the sections, and an area of $220 \times 220 \mu\text{m}$ was overlaid on the image. Alternate sections (35 μm each) of the entire SCN were examined bilaterally in 1- μm steps. Cells were considered double-labeled when both AR and the peptide or FOS signals occurred in the same cell for at least three consecutive 1- μm scans. In each animal, two sections of the hypothalamus containing the mid-SCN were sampled, and each of the four SCNs was independently counted (as described above). The average number of cells was computed for each animal, and then a group average was computed for each experimental group. Images were optimized for publication using Photoshop 7 (Adobe Systems, Mountain View, CA) and were adjusted only for brightness and contrast to enhance the signal-noise ratio.

Behavioral analysis—All behavioral analyses were carried out on at least 7 consecutive days of data at least 1 wk after any manipulation. Data were analyzed using Clocklab (Actimetrics Inc., Wilmette, IL) for Matlab (The MathWorks Inc., Natick, MA). Free-running period was calculated using a fast Fourier periodogram. Amount of daily activity was calculated as the number of wheel revolutions per day, averaged over 7 d. Onset of activity was defined as uninterrupted activity of at least 10 revolutions of the wheel per minute for 20 min. The precision of the daily onset of activity for each individual was calculated using the same 7-d window that was used in the activity amount analysis. The projected activity onset time for each day was calculated from the animal's free-running period. The difference between the actual and the projected onset time is reported as the precision. Thus, the smaller the precision value, the more precise is the animal's onset from day to day. Seven consecutive days of precision measurements were averaged for each animal. Sham GDX animals were included in the analysis of the intact group, and animals bearing blank capsule were included in the analysis of the GDX group, because no differences were found when quantified separately.

Statistics—All data are presented as mean \pm sem. Data for each experiment were analyzed using a one-way ANOVA (Sigma Stat; SPSS Inc., Chicago, IL). Results were considered statistically significant at $P < 0.05$. All significant main effects were further analyzed using a Tukey honest significant difference procedure.

Results

GDX alters circadian locomotor activity, whereas testosterone replacement reinstates circadian behavior in male mice

Given the dramatic effects of androgenic hormones on the SCN, we repeated the behavioral studies undertaken by Daan and colleagues (18) on C57BL/6 male mice over 30 yr ago. We replicated and extended this work by examining the effects of DHT and by using computer-assisted analyses not available earlier. The effects of GDX and androgen replacement on circadian patterns of locomotor activity in male mice are shown in Fig. 1, with detailed analyses in Table 1. In DD, within days of GDX, the circadian period is lengthened (24.21 ± 0.07 h; $P < 0.05$; $F = 15.63$), precision of activity onset is severely reduced (from 0.18 to 1.5 h; $P < 0.01$; $F = 66.00$), activity bout length (α) is reduced (1.94 ± 0.27 h; $P < 0.05$; $F =$

27.5), and dramatically, the animal no longer runs in the wheel at the predicted onset of subjective night, whereas the offset bout is unchanged (Fig. 1, A and B, and Table 1). After replacement with TP or DHT, the onset of the nightly activity bout is restored in phase with the projected onset, and the period and precision are restored to the precastration range (Fig. 1, C and D, respectively, and Table 1). TP (Fig. 1C) but not DHT (Fig. 1D) restores the amount of activity to precastration levels, although DHT does increase amount of activity over levels seen in castrates.

AR is highly localized in the SCN

Single-label ICC with an anti-AR antibody indicates that AR is strongly expressed within the SCN and is highly localized to the ventrolateral core aspect of the nucleus, with sparse staining in the dorsomedial shell region (Fig. 2). To confirm and extend these results, the AR transgenic mouse was examined. This mouse makes use of a dual reporter system, driven by the AR, in which a lacZ reporter is targeted to the nucleus, whereas a PLAP reporter is incorporated into all cellular membranes (26). As with the AR antibody, β -galactosidase staining reveals dense nuclear staining in the ventrolateral core SCN region (Fig. 3A). PLAP, which is incorporated into the cell membrane and permits visualization of soma and processes, shows that the greatest density of fibers occurs within the core SCN, with some fiber tracts apparently emanating dorsally from this part of the SCN (Fig. 3B).

To further delineate AR localization, we used confocal microscopy and double-label ICC to examine the coexpression of AR with GRP (Fig. 3C), AVP (Fig. 3D), and VIP (Fig. 3E). The results indicate that the majority of AR cells coexpress GRP (~58%), whereas only 3% coexpress VIP, and fewer than 2% express AVP (Fig. 4A). Conversely, almost all GRP cells (>85%), a small proportion of VIP cells (~12%), and few AVP cells (<7%) coexpress AR (Fig. 4B).

AR expression is not rhythmic in a LD cycle or in constant conditions

To evaluate the effect of a LD cycle or DD on SCN AR expression, Western blotting was used. In lysates of micro-dissected SCN from animals housed in LD or DD, no significant differences in AR protein expression levels across time were revealed (Fig. 5). The lower levels of AR expression observed at both ZT/CT20 and ZT/CT0 did not reach statistical significance ($P > 0.05$; Fig. 5A). ICC analysis of SCN AR expression at ZT0 and ZT12 (Fig. 5B) again indicated no statistically significant differences at these two time points, confirming the Western blot analysis.

GDX reduces SCN AR cell number, whereas replacement with testosterone restores AR levels

Using ICC, we next compared SCN AR-positive cell numbers in INT, GDX, and GDX+TP animals (Fig. 6). The number of AR-positive nuclei was greatly reduced from INT levels 7 d after GDX, whereas 7 d of TP replacement restored SCN AR levels to that of INT males.

AR cells express light-induced FOS, and this response is reduced after GDX but restored after DHT replacement

Given the anatomical localization of AR within light-responsive neurons of the ventrolateral core SCN, we examined the coexpression of AR and FOS after a 30-min phase-delaying light pulse at CT13.5, because the effects of GDX on behavior are most pronounced in the early night. About half of the SCN AR cells ($53 \pm 4\%$) coexpress FOS, and the majority of FOS cells express AR ($66 \pm 9\%$) at the 60-min post-stimulation time point examined in this study (Fig. 7).

To determine the effects of GDX on light-induced SCN FOS expression, INT, GDX, and GDX+DHT animals housed in DD for 2 d were exposed to a light pulse at either delay or advance phases of their circadian cycle. At both time points (Fig. 8), SCN FOS was significantly decreased ($P < 0.05$) in GDX animals when compared with intact controls, whereas GDX+DHT animals showed a restoration of FOS to levels seen in INT animals (not significantly different from INT, $P > 0.05$).

Discussion

It is well known that the SCN regulates the rhythmic secretion of gonadal androgens, and although there have been reports of sparse and/or scattered AR in other species (rat, baboon, rhesus, ferret, and human) (21–25), we now extend this to mouse and further show densely packed AR-containing cells that are highly localized to a specific functional subdivision of the SCN. Thus, rhythmic testosterone secretion is regulated by the brain clock. In turn, testosterone can act directly on AR receptors in the SCN and change the functioning of this master circadian clock (Fig. 9). These results support the notion of a neuroendocrine feedback loop in the circadian system (30).

Previous reports of scattered AR in various species (21–25) may represent true differences from mice. Alternatively, it is possible that the highly localized AR expression of the small region of the core SCN was missed in these earlier works, because many of the studies were done before the functional significance of the two SCN divisions was understood (6, 31).

Although AR expression is not limited to GRP-containing cells, almost all GRP cells contain AR. Several lines of evidence point to the significance of GRP in the synchronization of the individual oscillator phase. Electrical rhythmicity in the SCN can be restored in brain slices harvested from behaviorally arrhythmic mice lacking the VIP receptor (VPAC2) (32) by application of GRP, and this effect is blocked by treatment with a GRP receptor (GRPr) antagonist (33). Thus, GRP can resynchronize the network of cellular oscillators within the SCN, restoring SCN function. Importantly, GRP is also involved in photic phase resetting. The GRPr is expressed primarily in the rhythmic dorsomedial shell region of the SCN (34, 35). Mice lacking the gene for the GRPr show blunted phase shifts, and expression of light-induced *Per1* and *Per2* is decreased in the SCN (35). The localization of AR in GRP neurons is important, especially when one considers GRP's role in SCN responses to light, intra-SCN communication, and synchronization of SCN oscillator networks. Consistent with these studies, the present results show that castration reduces FOS expression in response to light pulses in both early and late subjective night. Likewise, the loss of coherence in locomotor activity after castration suggests that gonadal steroid feedback onto GRP cells may be required to coordinate individual SCN oscillators.

An important new finding is that AR cells of the SCN express FOS after photic stimulation, and FOS expression is significantly reduced in GDX animals, at both the phase-advance and phase-delay time points. This response is restored after DHT replacement. The androgenic effect may be directly on the SCN or an indirect effect on the retina (36). Thus, directly or indirectly, the SCN can act as an integration site for circadian, photic, and hormonal signals, providing a site of common action for circadian and environmental stimuli.

Mechanisms of AR action on cell physiology

There are myriad pathways by which androgenic hormones could influence SCN function through the AR. As is true for most other nuclear hormone receptors, unliganded AR is present in the cytoplasm and upon activation is translocated to the nucleus (37). The AR, together with steroid receptor coactivators, interacts with the androgen response element, one of many different hormone-responsive elements, on specific genes to alter

transcriptional regulation of a target (38, 39). Androgens can also engage other intracellular signaling pathways. In neurons, androgens can activate the MAPK/ERK pathway (40), a rapid signaling pathway implicated in SCN function. In the SCN, the MAPK/ERK pathway is involved in the neural and behavioral responses to a phase-shifting light pulse (reviewed in Ref. 41). Thus, AR activation within SCN cells is in a position to impact fast cellular processes as well as slower responses involving regulation of gene transcription.

Potential significance for models of SCN function

By studying a mouse in which neuronal membranes of AR cells are labeled, the present results demonstrate previously unknown aspects of the connectivity of AR-containing SCN cells. We show that the fiber plexus arising from AR cells is dense in the ventrolateral core region and sparse in the dorsomedial shell region and has some projections that course dorsally. Such results are consistent with previous observations that retinorecipient SCN neurons project directly to both dorsomedial shell and to extra-SCN targets (42–44). This projection pattern is consistent with a role in synchronizing activity of neurons in the ventrolateral core as well as relaying information to target sites in extra-SCN regions. However, tracking the projections of SCN-specific AR cell fiber bundles will prove difficult using only this method because of the density of AR cell fibers present in the hypothalamus, particularly from the anterior hypothalamus. A dual-track tracing technique may prove helpful in this case.

The notion that the SCN is made up of two coupled oscillators is a recurrent theme that emerges from behavioral studies. In the 1950s, Jürgen Aschoff described the basic two-peak pattern of locomotor activity as a persistent property of the circadian oscillator system in most species, and indicated that “it is by far the most common pattern” (cited in Ref. 45). This concept was elaborated in a mutually coupled oscillator model comprising an evening (E, beginning of night) and morning (M, end of night) oscillator (20). The E and M model suggests that a consolidated bout of nightly activity results from the coupling of these two oscillating components of the SCN (46). The work of Daan *et al.* (18) as well as our own replication and extension (Fig. 1) show that the early evening bout of activity is androgen dependent.

Recall that gonadectomy, with the consequent changes in SCN AR cells, eliminates the early night activity (the E-oscillator) component but has no effect on the late night activity interval (the M-oscillator component) (15) (Fig. 1), indicating that the former is dependent on the presence of circulating androgens. We propose that the AR cells differentially signal to the E- and M-oscillator population of the SCN. In this view, the E and M oscillators are parts of separable intra-SCN circuits. In nature, such androgenic effects may be important in determining the phase relationship of daily activity to seasonal changes in the time of dawn and dusk, such as are seen under various photoperiodic conditions (47–49). Although the gonadal axis of the mouse does not respond to day-length cues, there are seasonal changes in response to temperature and food availability in nature (50). The laboratory mouse SCN responds to changes in day length (51), and coding for photoperiod in the mouse brain clock involves plasticity in SCN networks (52). Moreover, it has been suggested that latent reproductive photoperiodism may remain in this species (53, 54).

SCN-dependent and -independent behaviors

Previous studies of androgenic effects on circadian responses suggest that the effects reported here can be attributed to actions directly on the SCN and on extra-SCN sites. Period, precision, and organization of daily activity are thought to be regulated by the SCN, whereas overall amount or amplitude of activity may not have a basis in the master circadian clock (20, 55). The present results show that replacement with either TP or DHT restores the

period, precision, and overall structure of nocturnal locomotor activity in GDX male mice, showing that these aspects of circadian behavior can be modulated by androgens. This is consistent with evidence showing that photoperiodic castration of male hamsters leads to alterations in the precision and organization of circadian activity (19). Our finding showing that both TP and nonaromatizable DHT reinstate SCN-based aspects of circadian behavior (period and precision) are consistent with earlier data showing that estradiol does not affect circadian period in male hamsters (56).

It is well known that gonadal hormones act on extra-SCN loci and that the AR is widely distributed in the rodent brain (57). The present findings that TP but not DHT restores amount of activity in GDX mice agrees with previous data. *In vivo*, TP can be converted to estradiol by the cytochrome p450 aromatase enzyme, whereas DHT is a nonaromatizable androgen. Thus, it is possible that the TP effect on total activity may be through its conversion to estradiol. Estradiol modulates overall locomotor activity levels in males (58, 59), with the medial preoptic area implicated as a site of action (60). Such extra-SCN estrogenic effects may be responsible for the increase in the amount of daily activity. This is also important when considering that the SCN lacks classical estrogen receptors (ER α and ER β), although very low levels of ER β peptide has been shown in the mouse SCN (61). Interestingly, there is evidence to suggest that ER α -containing cells within anterior hypothalamic sites, such as the medial preoptic area, may project to the SCN (62), although the magnitude and significance of these dispersed inputs remain unclear.

Summary

There is substantial evidence of androgenic effects on circadian activity, although direct effects on the SCN have not been well investigated. Our findings suggest that in the mouse, the SCN provides a neural substrate for a hypothalamic neuroendocrine loop whereby androgens can alter circadian behavior. AR is expressed in the SCN brain clock, where its expression is modulated by plasma testosterone levels but not by the LD cycle. SCN AR cells also respond to photic stimuli, indicating that these inputs converge on the same cells. Thus, the SCN regulates rhythmic gonadal hormone secretion, whereas androgens alter circadian behavior (18) (present results, Fig. 1 and Table 1) and SCN responses to light. Given the presence of AR in the human SCN (24) and the changes in hormone status and circadian rhythms in aging and depression, understanding the modulation of circadian function by androgens through a potential SCN site of action will prove a useful model.

Acknowledgments

We thank Drs. Joseph LeSauter, Lance Kriegsfeld, Russell Romeo, and Lily Yan for comments on previous versions of this manuscript.

This work was supported by the Natural Sciences and Engineering Research Council of Canada to I.N.K. and the National Institutes of Health (NS37919) to R.S. We also acknowledge the Confocal Microscopy Facility at Barnard College, supported by NSF DBI320988. Barnard College provided support for J.S.

Abbreviations

AR	Androgen receptor
AVP	arginine vasopressin
CT	circadian time
DD	constant darkness
DHT	dihydrotestosterone

E	evening
ER	estrogen receptor
GFP	green fluorescent protein
GRP	gastrin-releasing peptide
GRPr	GRP receptor
ICC	immunocytochemistry
INT	intact
ir	immunoreactivity
12:12 LD	12-h light, 12-h dark cycle
M	morning
PB	phosphate buffer
PLAP	placental alkaline phosphatase
SCN	suprachiasmatic nuclei
TP	testosterone propionate
VIP	vasoactive intestinal polypeptide
ZT	zeitgeber time

References

1. Welsh DK, Logothetis DE, Meister M, Reppert SM. Individual neurons dissociated from rat suprachiasmatic nucleus express independently phased circadian firing rhythms. *Neuron*. 1995; 14:697–706. [PubMed: 7718233]
2. Yamaguchi S, Isejima H, Matsuo T, Okura R, Yagita K, Kobayashi M, Okamura H. Synchronization of cellular clocks in the suprachiasmatic nucleus. *Science*. 2003; 302:1408–1412. [PubMed: 14631044]
3. Quintero JE, Kuhlman SJ, McMahan DG. The biological clock nucleus: a multiphasic oscillator network regulated by light. *J Neurosci*. 2003; 23:8070–8076. [PubMed: 12954869]
4. Yamazaki S, Numano R, Abe M, Hida A, Takahashi R, Ueda M, Block GD, Sakaki Y, Menaker M, Tei H. Resetting central and peripheral circadian oscillators in transgenic rats. *Science*. 2000; 288:682–685. [PubMed: 10784453]
5. Moore RY. Entrainment pathways and the functional organization of the circadian system. *Prog Brain Res*. 1996; 111:103–119. [PubMed: 8990910]
6. Abrahamson EE, Moore RY. Suprachiasmatic nucleus in the mouse: retinal innervation, intrinsic organization and efferent projections. *Brain Res*. 2001; 916:172–191. [PubMed: 11597605]
7. Yan L, Okamura H. Gradients in the circadian expression of *Per1* and *Per2* genes in the rat suprachiasmatic nucleus. *Eur J Neurosci*. 2002; 15:1153–1162. [PubMed: 11982626]
8. Nakamura W, Honma S, Shirakawa T, Honma K. Regional pacemakers composed of multiple oscillator neurons in the rat suprachiasmatic nucleus. *Eur J Neurosci*. 2001; 14:666–674. [PubMed: 11556891]
9. Hamada T, LeSauter J, Venuti JM, Silver R. Expression of *Period* genes: rhythmic and nonrhythmic compartments of the suprachiasmatic nucleus pacemaker. *J Neurosci*. 2001; 21:7742–7750. [PubMed: 11567064]
10. Jobst EE, Allen CN. Calbindin neurons in the hamster suprachiasmatic nucleus do not exhibit a circadian variation in spontaneous firing rate. *Eur J Neurosci*. 2002; 16:2469–2474. [PubMed: 12492442]

11. Yan L, Silver R. Differential induction and localization of mPer1 and mPer2 during advancing and delaying phase shifts. *Eur J Neurosci.* 2002; 16:1531–1540. [PubMed: 12405967]
12. Karatsoreos IN, Yan L, LeSauter J, Silver R. Phenotype matters: identification of light-responsive cells in the mouse suprachiasmatic nucleus. *J Neurosci.* 2004; 24:68–75. [PubMed: 14715939]
13. Morin LP. SCN organization reconsidered. *J Biol Rhythms.* 2007; 22:3–13. [PubMed: 17229920]
14. Roenneberg T, Kuehnle T, Pramstaller PP, Ricken J, Havel M, Guth A, Mewow M. A marker for the end of adolescence. *Curr Biol.* 2004; 14:R1038–R1039. [PubMed: 15620633]
15. Davis FC, Darrow JM, Menaker M. Sex differences in the circadian control of hamster wheel-running activity. *Am J Physiol.* 1983; 244:R93–R105. [PubMed: 6849422]
16. Wever RA. Properties of human sleep-wake cycles: parameters of internally synchronized free-running rhythms. *Sleep.* 1984; 7:27–51. [PubMed: 6718923]
17. Wever RA. Sex differences in human circadian rhythms: intrinsic periods and sleep fractions. *Experientia.* 1984; 40:1226–1234. [PubMed: 6500007]
18. Daan S, Damassa D, Pittendrigh CS, Smith ER. An effect of castration and testosterone replacement on a circadian pacemaker in mice (*Mus musculus*). *Proc Natl Acad Sci USA.* 1975; 72:3744–3747. [PubMed: 1059163]
19. Morin LP, Cummings LA. Effect of surgical or photoperiodic castration, testosterone replacement or pinealectomy on male hamster running rhythmicity. *Physiol Behav.* 1981; 26:825–838. [PubMed: 7267776]
20. Pittendrigh CS, Daan S. A functional analysis of circadian pacemakers in nocturnal rodents: pacemaker structure: a clock for all seasons. *J Comp Physiol A.* 1976; 106:333–355.
21. Wu SS, Nathanielsz PW, McDonald TJ. Immunocytochemical distribution of androgen receptors in the hypothalamus and pituitary of the fetal baboon in late gestation. *Brain Res Dev Brain Res.* 1995; 84:278–281.
22. Rees HD, Michael RP. Brain cells of the male rhesus monkey accumulate ^3H -testosterone or its metabolites. *J Comp Neurol.* 1982; 206:273–277. [PubMed: 7085933]
23. Zhou L, Blaustein JD, De Vries GJ. Distribution of androgen receptor immunoreactivity in vasopressin- and oxytocin-immunoreactive neurons in the male rat brain. *Endocrinology.* 1994; 134:2622–2627. [PubMed: 8194487]
24. Fernandez-Guasti A, Kruijver FP, Fodor M, Swaab DF. Sex differences in the distribution of androgen receptors in the human hypothalamus. *J Comp Neurol.* 2000; 425:422–435. [PubMed: 10972942]
25. Kashon ML, Arbogast JA, Sisk CL. Distribution and hormonal regulation of androgen receptor immunoreactivity in the forebrain of the male European ferret. *J Comp Neurol.* 1996; 376:567–586. [PubMed: 8978471]
26. Shah NM, Pisapia DJ, Maniatis S, Mendelsohn MM, Nemes A, Axel R. Visualizing sexual dimorphism in the brain. *Neuron.* 2004; 43:313–319. [PubMed: 15294140]
27. Wersinger SR, Haisenleder DJ, Lubahn DB, Rissman EF. Steroid feedback on gonadotropin release and pituitary gonadotropin subunit mRNA in mice lacking a functional estrogen receptor α . *Endocrine.* 1999; 11:137–143. [PubMed: 10709760]
28. Lindzey J, Wetsel WC, Couse JF, Stoker T, Cooper R, Korach KS. Effects of castration and chronic steroid treatments on hypothalamic gonadotropin-releasing hormone content and pituitary gonadotropins in male wild-type and estrogen receptor- α knockout mice. *Endocrinology.* 1998; 139:4092–4101. [PubMed: 9751487]
29. Lu SF, McKenna SE, Cologer-Clifford A, Nau EA, Simon NG. Androgen receptor in mouse brain: sex differences and similarities in autoregulation. *Endocrinology.* 1998; 139:1594–1601. [PubMed: 9528939]
30. Bell-Pedersen D, Cassone VM, Earnest DJ, Golden SS, Hardin PE, Thomas TL, Zoran MJ. Circadian rhythms from multiple oscillators: lessons from diverse organisms. *Nat Rev Genet.* 2005; 6:544–556. [PubMed: 15951747]
31. Antle MC, Silver R. Orchestrating time: arrangements of the brain circadian clock. *Trends Neurosci.* 2005; 28:145–151. [PubMed: 15749168]

32. Aton SJ, Colwell CS, Harmar AJ, Waschek J, Herzog ED. Vasoactive intestinal polypeptide mediates circadian rhythmicity and synchrony in mammalian clock neurons. *Nat Neurosci.* 2005; 8:476–483. [PubMed: 15750589]
33. Brown TM, Hughes AT, Piggins HD. Gastrin-releasing peptide promotes suprachiasmatic nuclei cellular rhythmicity in the absence of vasoactive intestinal polypeptide-VPAC2 receptor signaling. *J Neurosci.* 2005; 25:11155–11164. [PubMed: 16319315]
34. Karatsoreos IN, Romeo RD, McEwen BS, Silver R. Diurnal regulation of the gastrin-releasing peptide receptor in the mouse circadian clock. *Eur J Neurosci.* 2006; 23:1047–1053. [PubMed: 16519669]
35. Aida R, Moriya T, Araki M, Akiyama M, Wada K, Wada E, Shibata S. Gastrin-releasing peptide mediates photic entrainable signals to dorsal subsets of suprachiasmatic nucleus via induction of Period gene in mice. *Mol Pharmacol.* 2002; 61:26–34. [PubMed: 11752203]
36. Wickham LA, Gao J, Toda I, Rocha EM, Ono M, Sullivan DA. Identification of androgen, estrogen and progesterone receptor mRNAs in the eye. *Acta Ophthalmol Scand.* 2000; 78:146–153. [PubMed: 10794246]
37. Roy AK, Tyagi RK, Song CS, Lavrovsky Y, Ahn SC, Oh TS, Chatterjee B. Androgen receptor: structural domains and functional dynamics after ligand-receptor interaction. *Ann NY Acad Sci.* 2001; 949:44–57. [PubMed: 11795379]
38. Geserick C, Meyer HA, Haendler B. The role of DNA response elements as allosteric modulators of steroid receptor function. *Mol Cell Endocrinol.* 2005; 236:1–7. [PubMed: 15876478]
39. Geserick C, Meyer HA, Barbulescu K, Haendler B. Differential modulation of androgen receptor action by deoxyribonucleic acid response elements. *Mol Endocrinol.* 2003; 17:1738–1750. [PubMed: 12791770]
40. Nguyen TV, Yao M, Pike CJ. Androgens activate mitogen-activated protein kinase signaling: role in neuroprotection. *J Neurochem.* 2005; 94:1639–1651. [PubMed: 16011741]
41. Coogan AN, Piggins HD. MAP kinases in the mammalian circadian system: key regulators of clock function. *J Neurochem.* 2004; 90:769–775. [PubMed: 15287881]
42. Kriegsfeld LJ, Leak RK, Yackulic CB, LeSauter J, Silver R. Organization of suprachiasmatic nucleus projections in Syrian hamsters (*Mesocricetus auratus*): an anterograde and retrograde analysis. *J Comp Neurol.* 2004; 468:361–379. [PubMed: 14681931]
43. De la Iglesia HO, Schwartz WJ. A subpopulation of efferent neurons in the mouse suprachiasmatic nucleus is also light responsive. *Neuroreport.* 2002; 13:857–860. [PubMed: 11997701]
44. Leak RK, Card JP, Moore RY. Suprachiasmatic pacemaker organization analyzed by viral transynaptic transport. *Brain Res.* 1999; 819:23–32. [PubMed: 10082857]
45. Aschoff J. Circadian activity pattern with two peaks. *Ecology.* 1966; 47:657–662.
46. Daan S, Albrecht U, van der Horst GT, Illnerova H, Roenneberg T, Wehr TA, Schwartz WJ. Assembling a clock for all seasons: are there M and E oscillators in the genes? *J Biol Rhythms.* 2001; 16:105–116. [PubMed: 11302553]
47. van Oort BE, Tyler NJ, Gerkema MP, Folkow L, Blix AS, Stokkan KA. Circadian organization in reindeer. *Nature.* 2005; 438:1095–1096. [PubMed: 16371996]
48. Hofman MA. The brain's calendar: neural mechanisms of seasonal timing. *Biol Rev Camb Philos Soc.* 2004; 79:61–77. [PubMed: 15005173]
49. Gorman MR, Freeman DA, Zucker I. Photoperiodism in hamsters: abrupt versus gradual changes in day length differentially entrain morning and evening circadian oscillators. *J Biol Rhythms.* 1997; 12:122–135. [PubMed: 9090566]
50. Bronson FH. The reproductive ecology of the house mouse. *Q Rev Biol.* 1979; 54:265–299. [PubMed: 390600]
51. Inagaki N, Honma S, Ono D, Tanahashi Y, Honma K. Separate oscillating cell groups in mouse suprachiasmatic nucleus couple photoperiodically to the onset and end of daily activity. *Proc Natl Acad Sci USA.* 2007; 104:7664–7669. [PubMed: 17463091]
52. VanderLeest HT, Houben T, Michel S, Deboer T, Albus H, Vansteensel MJ, Block GD, Meijer JH. Seasonal encoding by the circadian pacemaker of the SCN. *Curr Biol.* 2007; 17:468–473. [PubMed: 17320387]

53. Nelson RJ, Shiber JR. Photoperiod affects reproductive responsiveness to 6-methoxy-2-benzoxazolinone in house mice. *Biol Reprod.* 1990; 43:586–591. [PubMed: 2289012]
54. Nelson RJ. Photoperiodic responsiveness in house mice. *Physiol Behav.* 1990; 48:403–408. [PubMed: 2267249]
55. Daan S, Oklejewicz M. The precision of circadian clocks: assessment and analysis in Syrian hamsters. *Chronobiol Int.* 2003; 20:209–221. [PubMed: 12723881]
56. Zucker I, Fitzgerald KM, Morin LP. Sex differentiation of the circadian system in the golden hamster. *Am J Physiol.* 1980; 238:R97–R101. [PubMed: 7356053]
57. Stumpf, WE.; Grant, LD. Anatomical neuroendocrinology. International Conference on Neurobiology of CNS-Hormone Interactions; Chapel Hill, NC. 1974. p. 472
58. Ogawa S, Chan J, Gustafsson JA, Korach KS, Pfaff DW. Estrogen increases locomotor activity in mice through estrogen receptor α : specificity for the type of activity. *Endocrinology.* 2003; 144:230–239. [PubMed: 12488349]
59. Morgan MA, Schulkin J, Pfaff DW. Estrogens and non-reproductive behaviors related to activity and fear. *Neurosci Biobehav Rev.* 2004; 28:55–63. [PubMed: 15036933]
60. Fahrbach SE, Meisel RL, Pfaff DW. Preoptic implants of estradiol increase wheel running but not the open field activity of female rats. *Physiol Behav.* 1985; 35:985–992. [PubMed: 4095192]
61. Mitra SW, Hoskin E, Yudkovitz J, Pear L, Wilkinson HA, Hayashi S, Pfaff DW, Ogawa S, Rohrer SP, Schaeffer JM, McEwen BS, Alves SE. Immunolocalization of estrogen receptor β in the mouse brain: comparison with estrogen receptor α . *Endocrinology.* 2003; 144:2055–2067. [PubMed: 12697714]
62. De La Iglesia HO, Blaustein JD, Bittman EL. Oestrogen receptor- α -immunoreactive neurones project to the suprachiasmatic nucleus of the female Syrian hamster. *J Neuroendocrinol.* 1999; 11:481–490. [PubMed: 10444305]
63. Kalsbeek A, Palm IF, La Fleur SE, Scheer FA, Perreau-Lenz S, Ruiters M, Kreier F, Cailotto C, Buijs RM. SCN outputs and the hypothalamic balance of life. *J Biol Rhythms.* 2006; 21:458–469. [PubMed: 17107936]

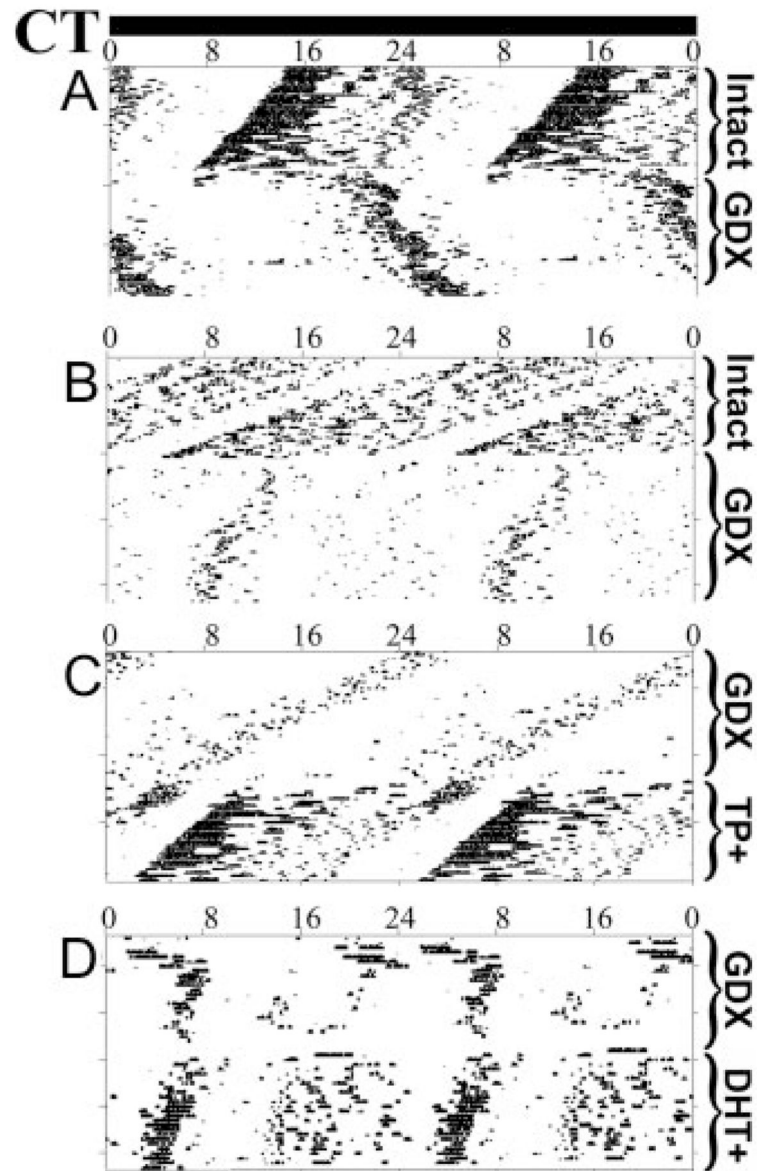


Fig. 1. Wheel-running activity of male mice housed in DD, after various hormonal manipulations for four representative individuals. CT is indicated across the *top* and double-plotted for ease of reference. Successive days are plotted downwards. A and B, Free-running records of INT animals and the effect of GDG on locomotor activity patterns; C, GDG animal free-running and then replaced with a SILASTIC brand capsule containing TP; D, GDG animal free-running and then replaced with a SILASTIC brand capsule containing DHT.

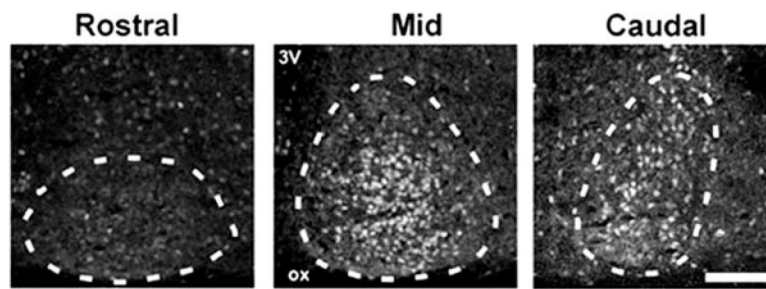


Fig. 2. Photomicrographs depicting AR-ir in coronal sections in rostral (*left*), mid (*center*), and caudal (*right*) aspects of the SCN showing that AR-ir cells are concentrated within the mid and caudal aspects of the SCN. *Dotted lines* delineate the extent of the SCN as defined by AVP double labeling (not shown). *Scale bar*, 150 μ m. ox, Optic chiasm; 3V, third ventricle.

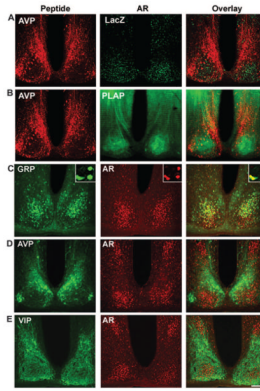


Fig. 3.

A and B, Photomicrographs depicting lacZ and PLAP reporters in the mid-SCN of AR-transgenic mice. The *left column* shows AVP, the *middle column* shows an AR reporter, and the *right column* shows the overlay. AVP (red) is used as a marker for the extent of the SCN. LacZ (A, green) staining confirms the results in Fig. 2, indicating that AR cells are highly concentrated in the ventrolateral core SCN. PLAP staining (B, green) also confirms the previous results and shows fibers of AR-containing cells fill the core SCN and are less dense in the dorsomedial shell region delineated by the AVP staining. There is a dense fiber plexus within the SCN, and efferents appear to exit dorsally from the nucleus. The area of intense PLAP staining dorsal to the SCN are AR fibers in the bed nucleus of the stria terminalis. C–E, Colocalization studies made use of double-labeled immunofluorescence in 35- μm coronal sections, stained for GRP (C), AVP (D), and VIP (E). The *left column* shows the peptide, the *middle column* shows AR, and the *right column* shows the overlay. Scale bar, 150 μm . ox, Optic chiasm; 3V, third ventricle. Inset on upper right of each panel in upper row shows a high-powered image from a 1- μm confocal scan.

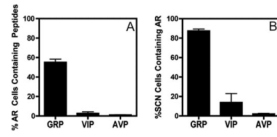


Fig. 4. Quantification of the colocalization experiments shown in Fig. 3, C–E. A, Percentage of AR cells that contain GRP, VIP, and AVP; B, percentage of peptide-containing cells that are positive for AR.

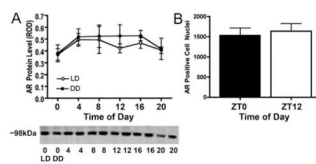


Fig. 5. A, Western blot analysis of AR in the SCN over time in DD (●) and in LD (○). Representative gel shown below, with alternate lanes showing LD and DD. B, quantification of the number of AR-positive nuclei per SCN at ZT0 and ZT12. There were no statistically significant differences.

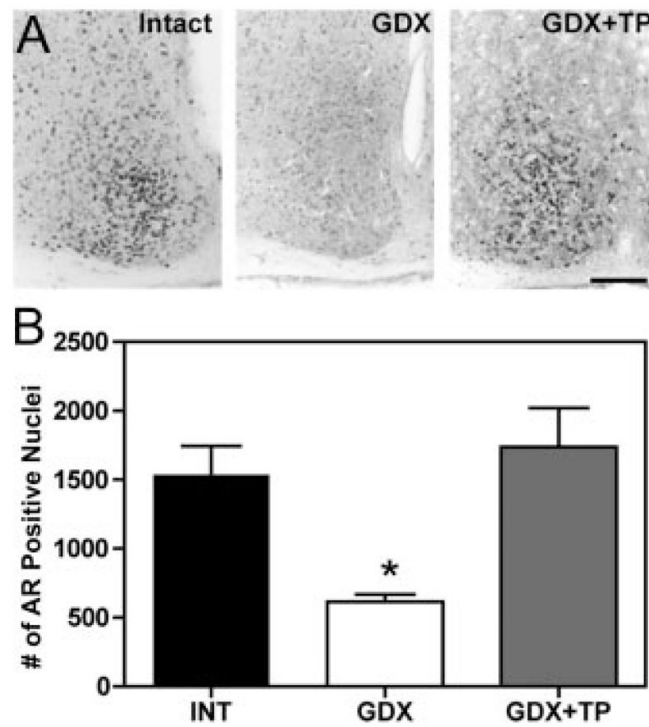


Fig. 6.

A, Photomicrographs depict AR-ir in coronal sections of the SCN of intact (*left*), GDX (*center*), and TP-treated GDX (*right*) mice. *Scale bar*, 150 μ m. B, Histograms depict number of AR-ir nuclei in the SCN of intact, GDX, and TP-treated mice. The number of AR-ir nuclei decreases after GDX with a recovery to intact levels after TP treatment. *, $P < 0.05$.

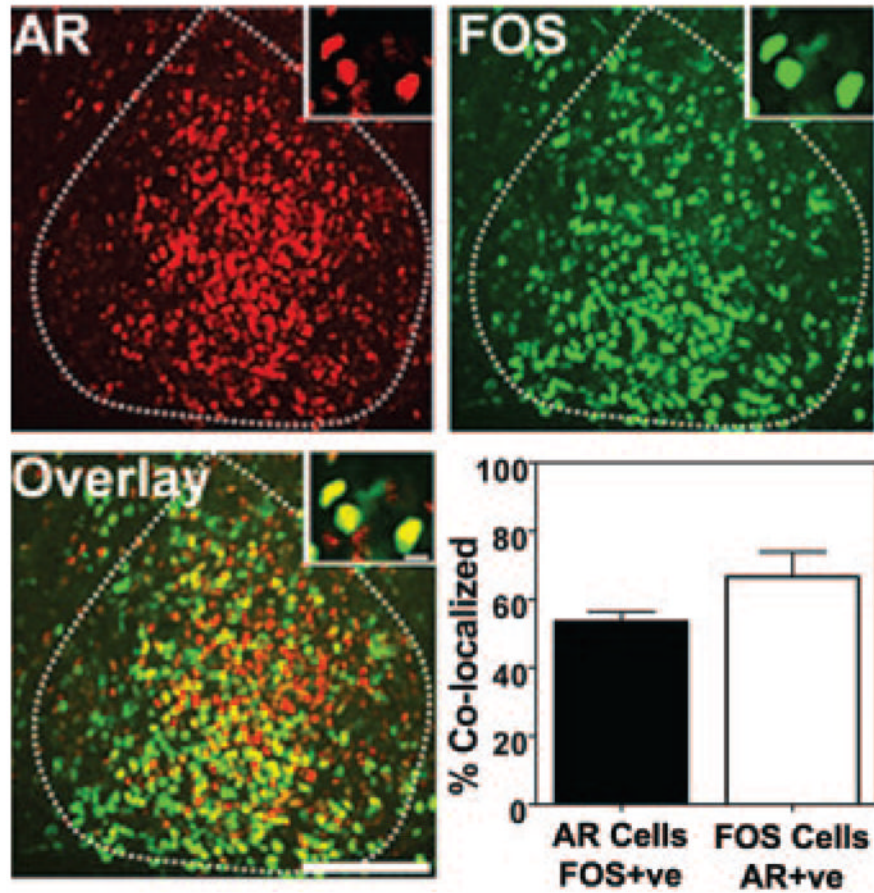


Fig. 7. Double-labeled immunofluorescence for AR (*red*), FOS (*green*), and the overlay in mid-SCN at 60 min after a 30-min light pulse at CT13.5. *Dashed line* indicates boundaries of the SCN. *Scale bar*, 150 μm . *Insets* show high-powered image of a 1- μm z-axis confocal scan. Graph shows percent colocalization of AR and FOS after the light pulse.

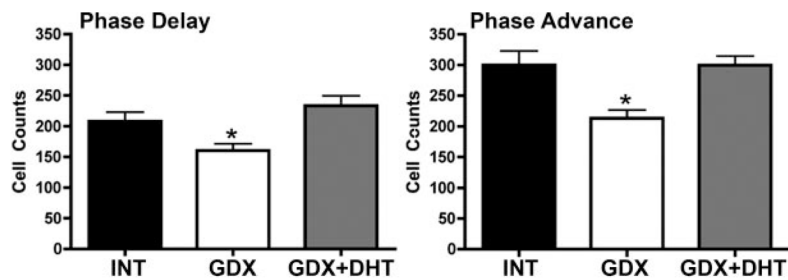


Fig. 8.

Quantification of the number of FOS cells after a light pulse in intact, GDX, and GDX +DHT animals at either the phase delay (CT13.5; *left*) or phase advance (CT21; *right*) phases of their circadian cycle. The number of FOS-ir cells decreases in GDX animals at both times (*, $P < 0.05$), whereas DHT treatment restores this response (not different from INT).

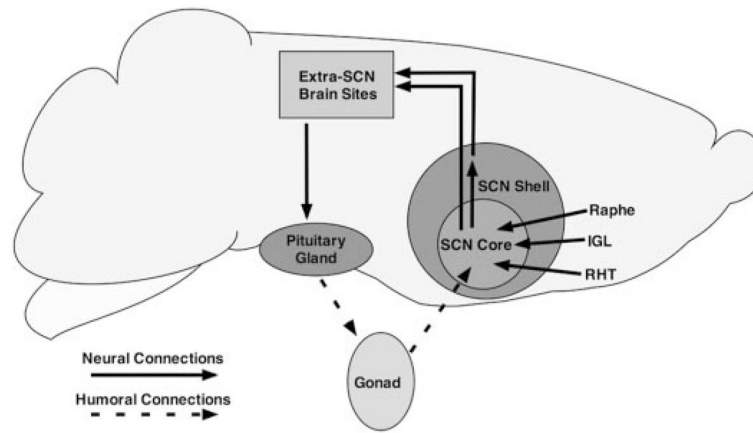


Fig. 9.

Schematic representation of the hypothalamic neuroendocrine loop completed by AR in the ventrolateral SCN core. The SCN projects to anterior hypothalamic neurosecretory cells, which project to the anterior pituitary (63). Pituitary tropic hormones are released into the general circulation to reach the gonads. In the male, testosterone in the blood reaches the SCN, binding to AR within the SCN, serving as an endocrine afferent input. Neural inputs from the retinohypothalamic tract (RHT), intergeniculate leaflet (IGL), and raphe nucleus also reach cells of the ventrolateral core SCN. Thus, endocrine and neural signals interact within the SCN to modulate circadian timing in the system.

TABLE 1
Effects of castration and androgen replacement on circadian locomotor rhythms in male mice

Group	n	Period (h ± sem)	Onset precision (h ± sem)	α Duration (h ± sem)	Total activity (daily turns)
Intact	14	23.65 ± 0.69	0.18 ± 0.04	13.85 ± 1.02	15,487.56 ± 1,086.5
GDX	14	24.21 ± 0.07 ^a	1.5 ± 0.49 ^a	1.94 ± 0.27 ^a	5,156.72 ± 1,017.24 ^a
GDX + TP	8	23.82 ± 0.23	0.20 ± 0.12	13.77 ± 1.78	15,564.36 ± 538.64
GDX + DHT	6	23.92 ± 0.42	0.22 ± 0.14	11.5 ± 2.57	10,382.73 ± 1,433.9 ^a

Measures of period, onset precision, and amplitude of circadian locomotor rhythmicity were measured in mice maintained in DD. Measures were taken from animals 7 d after GDX, 7 d after replacement with sc SILASTIC brand capsules bearing TP or dihydrotestosterone DHT, and intact animals. Period, precision, and amplitude were all affected by GDX, with all measures returning to near normal levels after systemic replacement.

^aSignificant difference from all other groups at $P < 0.05$.